DESIGN, OPERATION, AND INVESTIGATION OF AN INDUCTIVELY-DRIVEN, COAXIAL PULSED PLASMA THRUSTER

H. Kamhawi, P.J. Turchi, I.G. Mikellides, P.G. Mikellides
The Ohio State University
Columbus, Ohio USA

ABSTRACT

An Inverse-Pinch Coaxial Pulsed Plasma Thruster (PPT) has been designed and operated. This preliminary investigation operated the thruster at 15 J with a peak current of 20 Ka. Magnetic field mappings were performed at radial locations of 1.5 cm, 2 cm, and 3 cm and at azimuthal locations of 0°, 90°, and 180°. Results show that at the radial location of 1.5 cm there exists a non-symmetric current distribution with peak enclosed current values occurring at ignition locations.

INTRODUCTION

The Pulsed Plasma Thruster is exhibiting renewed interest for use in satellite station keeping, drag make-up, and orbit raising mainly because of its simplicity and robustness. Nevertheless, low energy rectangular PPT thrusters suffer from low thrust efficiencies ranging from 1.5% to 12%[1].

Recent experimental and numerical work[2,3] indicated that PPT's low efficiency is mainly attributed to poor mass utilization. Results indicate that only a small fraction of the total mass ablated is accelerated electromagnetically to high speeds (up to 30 km/s), while the majority of the ablated mass comes off the Teflon solid surface as neutrals and is accelerated gas-dynamically along the electrode channels with low speeds (< 3km/s). This poor mass utilization is mainly caused by the fact that the decomposed mass is far greater than the mass needed for electromagnetic acceleration. The main mechanism governing the generation of decomposed mass is the diffusion of heat from the high temperature arc discharge onto the solid Teflon surface. This heat causes the Teflon to depolymerize, dissociate, and partially ionize. Thus by determining, and controlling the shape and duration of the PPT discharge current which also governs and determines the magnetic field strength on the Teflon surface, attempts can be made to improve the mass utilization of PPT thrusters.

Recent numerical simulations[2] have indicated that to optimally utilize the ablated mass in rectangular geometry PPTs, the required current waveforms are characterized by prolonged duration or fast-rising high current levels both of which are not attainable due to circuit and available power limitations. These simulations found that having an axisymmetric 20 kA peak current with a rise time of 2 μsec current waveform in an Inverse-Pinch PPT at a Teflon propellant radius and gap of 1 cm can lead to efficient mass utilization.

This paper presents a preliminary investigation of the electrical characteristics and magnetic field distribution of an Inverse Pinch PPT.

EXPERIMENTAL FACILITIES AND INVERSE-PINCH PPT THRUSTER

The experimental investigation of the Inverse-Pinch PPT is performed at NASA Glenn Research Center (GRC) Electric Propulsion Laboratory, Cleveland, Ohio. Experiments are performed in the bell-shaped vacuum facility 54 (VACFAC 54). VACFAC 54 has an interior diameter of 51 cm and is 100 cm long. A 25 cm recess that is 15 cm long allows the roughing and oil diffusion pumps to evacuate the chamber to to pressures as low as $5X10^{-6}$ torr.

The Inverse-Pinch PPT schematic is presented in Figure 1. The capacitor used is a Maxwell Laboratory oil-filled 30 μf (actual 33.2 μf). The capacitor has a cylinderical metal case whose diameter is 8.4 cm and is 8.9 cm long. In addition,

the hot stud is located at the center of the cylinder and is surrounded by a ground ring. The ground ring has an inner diameter of 5.1 cm and an outer diameter of 6.35 cm. The capacitor is rated for a maximum voltage and current of 2000 volts and 25 Ka, respectively. A Rogowski coil is potted around the hot stud. This coaxial arrangement of the hot stud and the ground ring greatly simplified the design of the Inverse-Pinch PPT hot and ground transmission lines. The Aluminum ground transmission line has an inner diameter of 5.1 cm and an outer diameter of 6.35 cm; it is 12.4 cm long. At the end of the ground trasmission line the "nozzle shaped" electrode is attached. For the present design , its shape is depicted in Figure 1. The hot transmission line is comprised of two parts. The first is a 2.54 cm long brass piece with a diameter of 2.4 cm, it is attached directly into the capacitor's hot stud. The second part is the bottle-shaped Aluminum trasmission rod which is 8.84 cm long and has a diameter of 2.54 cm, its upper diameter is 1.25 cm and is 2.54 cm long for an exposed Teflon gap of 1 cm. The Teflon fuel annular is inserted into the the top of the Aluminum transmission line, it has an inner diameter of 1.25 cm, an outer diameter of 2 cm, and is 2.54 cm long. The exposed Teflon fuel height is 1 cm. The brass anode has a diameter of 2.4 cm.

Two RG-58 coaxial cable are used to initiate the PPT's discharge, they are powered by a Unison ignition exciter circuit that produces two ignition pulses. The output current from the ignition exciter circuit was measured and results indicate that the ignition pulses are simultaneous. The two igniting leads are placed 0.51 cm from the face of the Teflon surface. Figure 2 depicts a layout of the experimental setup.

EXPERIMENTAL DATA

Current Waveforms

The Rogowski loop used to monitor the PPT current is potted around the capacitor's hot stud, the Rogowski loop output was integrated with an RC integrator with an RC time constant of 56 μsec. To calibrate the Rogowski loop, a rectagular PPT was setup where a model 101 Pearson wide band current monitor can be used with the PPT's Rogowski coil to measure the PPT's current. The 0.01 volt/amp 1% accurate output of the Pearson current monitor was compared to the integrated Rogowki coil output, that resulted in a Rogowski coil calibration number of $1.152X10^4$ Amp/volts computed with an accuracy of 5%.

Current waveforms were recorded for capacitor energy levels of 5 J, 10 J , and 15 J corresponding to an initial charging voltage of 548 volts, 776 volts, and 952 volts, respectively . Results are presented in Figures 3 and 4 for Teflon fuel gap of 1 cm and 1.6 cm, respectively. In Figure 3, peak currents of 10.5 kA, 15.6 kA, and 20 kA, correspond to energy levels of 5 J, 10 J, and 15 J, respectively. Figure 3 indicates that there exists a 50% current reversal. In Figure 4, peak currents of 7.8 kA, 11.5 kA, and 15.2 kA, correspond to energy levels of 5 J, 10 J, and 15 J, respectively ; Figure 4 indicates that there exists a 33% current reversal. It is important to note here that peak currents are 25% lower for the 1.6cm Teflon gap when compared to the 1.0 cm Teflon gap . Comparing the experimental current waveforms to an output of an RLC circuit solver is used to obtain the Inverse Pinch PPT circuit parameters. Results show that for the 15 J 1 cm Teflon gap the circuit has a resistance of 15.7 mΩ and an inductance of 41.78 nH, whereas for the 1.6 cm Teflon gap the circuit has a resistance of 27.5 mΩ and an inductance of 51.26 nH.

Magnetic Field and Enclosed Current Mappings

Three magnetic probes are used to map the magnetic field and enclosed current contours in the interelectrode region and the PPT plume. The probes are made of 4 turns of 30 gauge magnetic wire, they have an inner diameter of 1 mm. The probes and the twisted pair of magnetic wire are enclosed in a pyrex tube which has an inner diameter of 1.4 mm and an outer diameter of 3 mm; the tube is 25 cm long and is closed at one end. At the tube open end the pair of magnetic twisted wire are connected to a RG-174U miniture coaxial cable. The output signals from all three probes are integrated via an RC integrator with a time constant

of 10 μsec. The probes are calibrated using a setup employing the Inverse Pinch PPT, the calibration numbers for probes 1, 2, and 3 are 2.36 Tesla/volt, 2.35 Tesla/volt, 2.36 Tesla /volt, respectively. The probes have an accuracy of ±13% and is mainly attributed to uncertainty in current measurement and probe positioning.

For magnetic field mapping, three magnetic probes were inserted simultenously at the same radial location but at azimuthal positions of 0°, 90°, and 180°; respectively. The 0° and 180° azimuthal positions are aligned with the two ignition cables that are used. The magnetic field mappings are performed at radial locations of 1.5 cm, 2 cm, and 3 cm at axial locations between 0 cm and 2 cm with increments of 0.2 cm. The probes are transversed between the 0 cm (at nozzle electrode surface) and 2 cm (exit plane location) via a computer-controlled stepper- motor powered motion table, the axial probe positioning is accurate to ±1 mm. It is important to note here that at a radial location of 3 cm the minimum axial location is 0.6 cm due to the curvuture of the nozzle. Figure 5, represents a typical magnetic probe output signal for all three probes.

Figure 6 presents the magnetic field distribution at a radial location of 1.5 cm for the 1 cm Teflon gap at an initial stored energy of 15 J. Results clearly show that the magnetic field distribution at the azimuthal locations of 0° and 180° is similar, whereas at the 90° azimuthal location the magnetic field strength is substantially lower. It is important to re- emphasize here that the 0° and 180° concide with the ignition cable locations. Calculating the enclosed current magnitude using

$$I_{encl} = \frac{B_\theta 2\pi r}{\mu} \qquad (1)$$

where B_θ is the magnetic field strength in Tesla, it is found that at an axial location of 0.6 cm at the 0° and 180° azimuthal locations the enclosed current is 20 kA, whereas at the 90° azimuthal location the enclosed current value is 7.4 kA. This indicates that there exists a nouniform current distribution at a radial location of 1.5 cm; this non-symmetric current distribution will result in non-uniform heat deposition into the Teflon surface and result in poor mass utilization. In addition, further analysis of Figure 6 indicates that the magnetic field strength decreases as the probes are moved away from the initial arc location.

Figures 7 and 8 show the magnetic field axial disrtidution for radial location of 2 cm and 3 cm, respectively. In both cases it is noted that at a given axial location , the magnetic field values at the different azimuthal locations are uniform. This indicated that as the probes are moved radially outward the plasma flow becomes more uniform as can be seen by inspecting Figures 7 and 8.

To study the effect of the ignition cable placement on the initial curent distribution, the Inverse Pinch PPT is operated with one ignition cable, the ignition cable is placed at the 0° azimuthal location. Figure 9 presents the magnetic field distribution for the 1 cm Teflon gap at a radial location of 2 cm. Results indicate that the magnetic field distribution is nonuniform. The enclosed current value at the zero axial location at 0° is 21 kA, while at the 90 ° and 180° locations the enclosed current value is approximately 14 kA. From earlier indications, this nonuniformity will be more severe at the smaller radial locations.

CONCLUSIONS

The experimental investigation of an Inverse-Pinch PPT is initiated. Operation at input energy of 15 J has produced a peak current of 20 Ka for Teflon gap of 1 cm. Magnetic field measurements were performed to examine axisymmetry characteristics and deduce current distribution. These preliminary results show that axisymmetry fails at the radial location(s) that coincides with that of the ignition. Further research will confirm consistency of the aforementioned observations and examine avenues to produce an azimuthally uniform current distribution. Partly, this can be accomplised by attempting to introduce a more azimuthally uniform ignition pulse and by studying the effects of different geometric variations on the PPT current distribution.

ACKNOWLEDGEMENTS

The authors acknowledge the support of the NASA Glenn Research Center. The assistance of the Mr. Eric Pencil is greatly appreciated.

REFERENCES

1. Burton, R.L., and Turchi, P.J., "Pulsed Plasma Thruster", Journal of Propulsion and Power, Vol. 14, No. 5, pp 716-735, Sep-Oct 1998

2. Mikellides, I.G., Turchi, P.J., "Optimization of Pulsed Plasma Thrusters in Rectangular and Coaxial Geometries", Pre-print IEPC Paper 99-211.

3. Turchi, P.J., "Directions for improving PPT Performance", Proceedings of the 25th International Electric Propulsion Conference, Vol. 1, Electric Rocket Propulsion Society, Worthington, OH, 1998, pp.251-258.

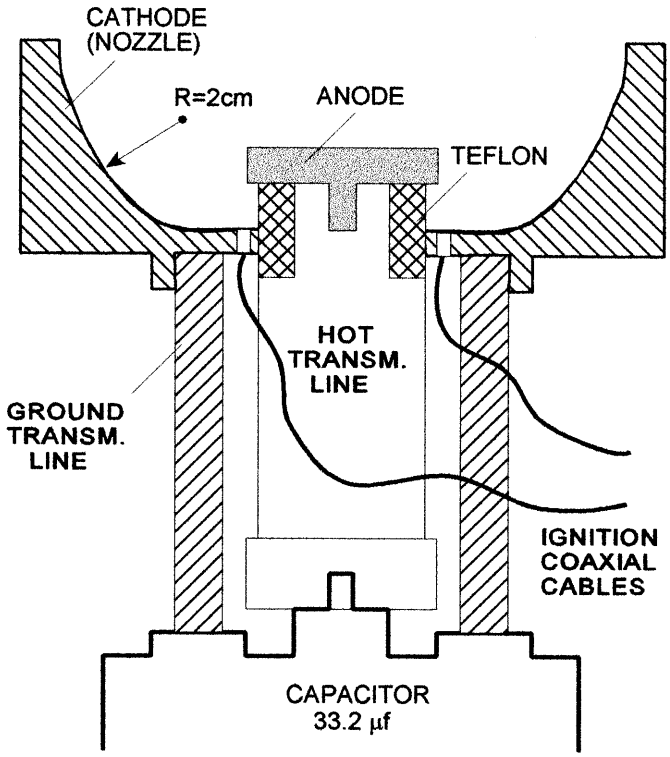

Figure 1: Schematic of Inverse Pinch PPT

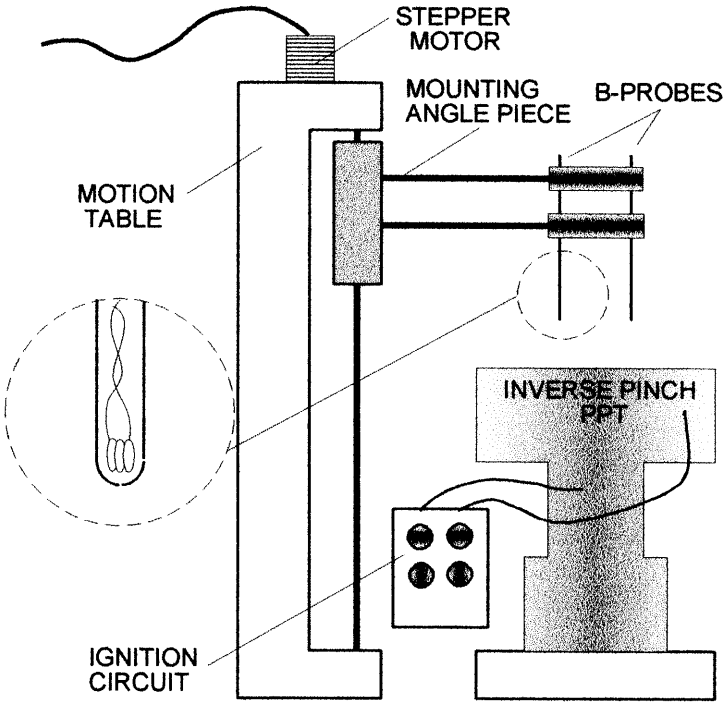

Figure 2: Experimental setup

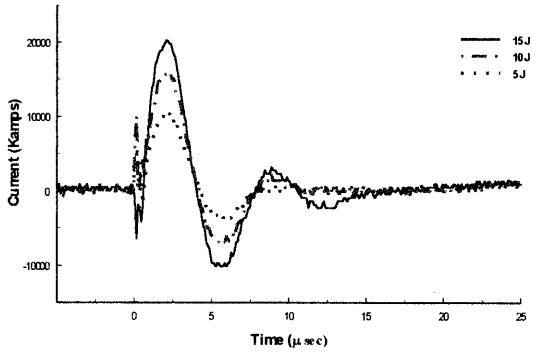

Figure 3: Current waveforms for the 1 cm Teflon gap at energy levels of 5 J, 10 J,and15J

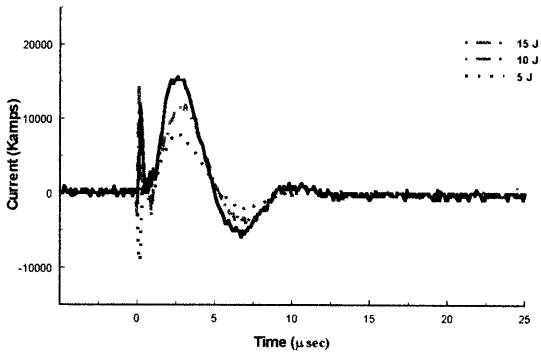

Figure 4: Current waveforms for the 1.6 cm Teflon gap at energy levels of 5 J, 10 J, and 15 J

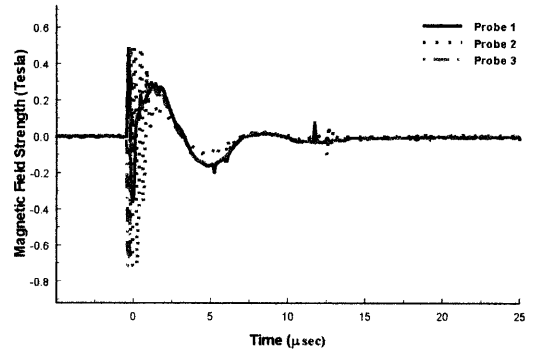

Figure 5: Magnetic field probe signals at r=1.5 cm at z=0.6 cm.

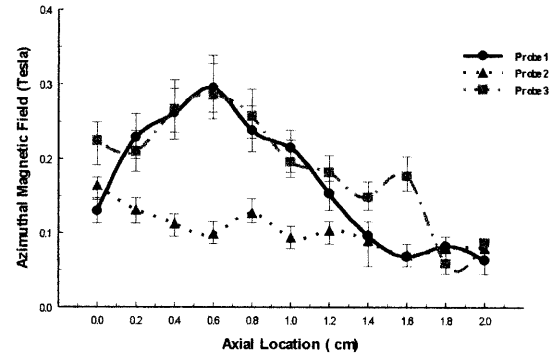

Figure 6: Magnetic field profiles for r=1.5 cm for energy level of 15 J

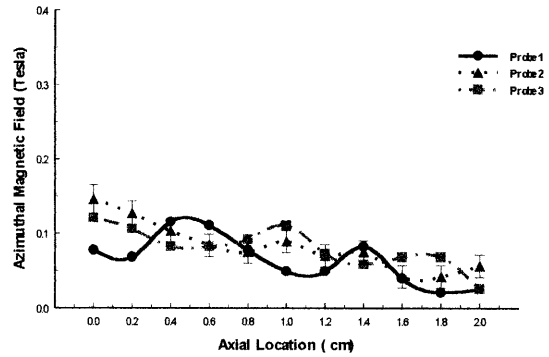

Figure 7: Magnetic field profiles for r=2 cm for energy level of 15 J

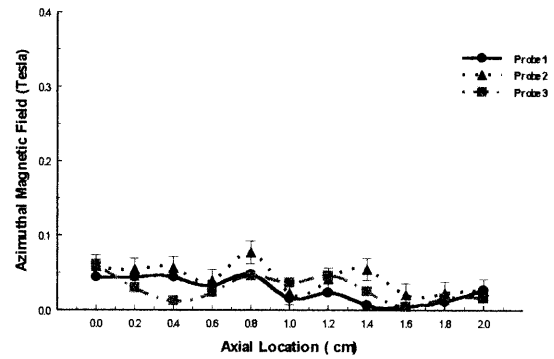

Figure 8: Magnetic field profiles at r=3 cm for energy level of 15 J

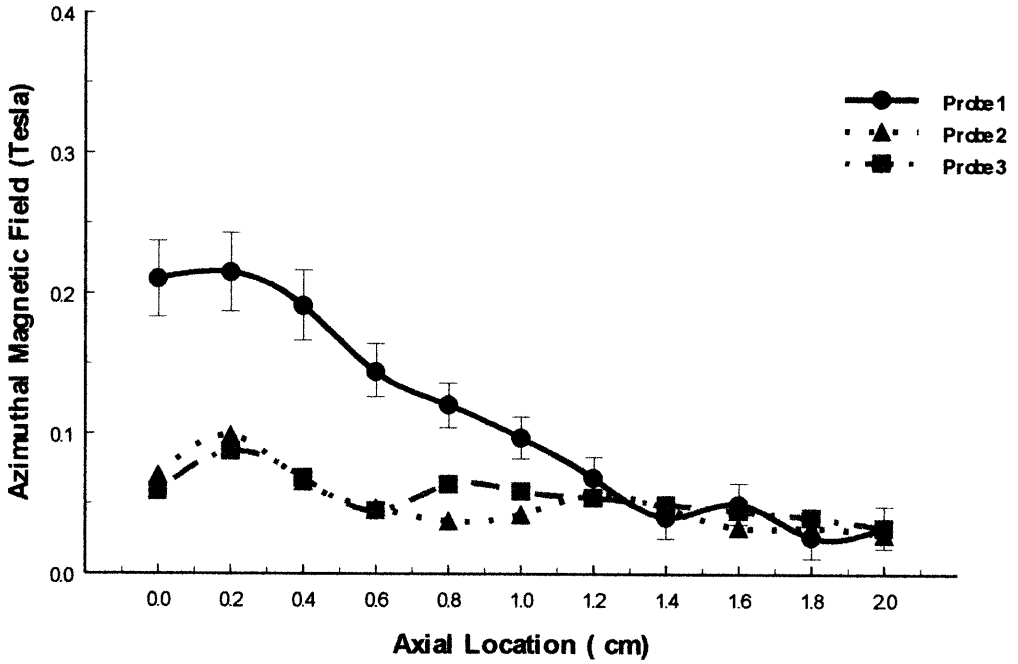

Figure 9: Magnetic field profiles at r=2 cm using one ignition source at probe 1 location for E= 15 J